Structural Insights from the Mo K-Edge X-ray Absorption Near Edge Structure of the Iron–Molybdenum Protein of Nitrogenase and Its Iron–Molybdenum Cofactor by Comparison with Synthetic Fe–Mo–S Clusters

S. D. Conradson,[1a] B. K. Burgess,[1b,f] W. E. Newton,[1c,g] Keith O. Hodgson,*[1a] J. W. McDonald,[1b] J. F. Rubinson,[1b] S. F. Gheller,[1b] L. E. Mortenson,[1d,h] M. W. W. Adams,[1d,h] P. K. Mascharak,[1e] W. A. Armstrong,[1e] and R. H. Holm[1e]

Contribution from the Department of Chemistry, Stanford University, Stanford, California 94305, the Department of Chemistry, Harvard University, Cambridge, Massachusetts 02138, the Battelle-C.F. Kettering Research Laboratory, Yellow Springs, Ohio 45387, the Western Regional Research Center, USDA-ARS, Albany, California 94710, the Department of Molecular Biology and Biochemistry, University of California at Irvine, Irvine, California 92717, and the Department of Biological Sciences, Purdue University, West Lafayette, Indiana 47907. Received April 15, 1985

Abstract: The Mo environment in the Fe–Mo–S cluster of nitrogenase has been examined by comparisons of the Mo K-edge X-ray absorption edge and near edge structure (collectively referred to herein as XANES) of *Clostridium pasteurianum* and *Azotobacter vinelandii* FeMo protein, as isolated FeMo cofactor (FeMoco), benzene thiol- and selenol-treated FeMoco, and a variety of synthetic Mo–S complexes and Fe–Mo–S clusters of known structure. There is a distinct correlation between the shapes of the absorption edge features (examined as second derivative absorbance curves) of the synthetic compounds and the environment of the nearest-neighbor atoms around the Mo atom. The significance of these results pertaining to the general problem of the interpretation of XANES spectra is discussed. The Mo XANES of the nitrogenase samples are quite similar to each other and to the XANES of cubane-type $MoFe_3S_4$ clusters possessing a MoS_3O_3 coordination unit. They are dissimilar to the XANES of all other types of synthetic compounds examined. The conclusion from these XANES studies is that the Mo site of the native cluster is approached in these synthetic clusters. This result is complementary to and consistent with, but independent of, results from Mo EXAFS studies.

The Mo atoms in the FeMo protein of nitrogenase are generally believed to be intimately involved in the catalytic cycle, if not (part of) the actual site of substrate binding and reduction.[2] Treatment of acid-denatured FeMo protein with NMF^3 releases molybdenum from the protein matrix in the form of the iron–molybdenum cofactor (FeMoco).[4] A variety of physical techniques applied to the FeMo protein and/or free FeMoco have shown that the cofactor is a Fe–Mo–S cluster. Results of many of these investigations have been summarized;[4c,5–8] note is made of certain more recent spectroscopic studies.[9] The collective spectroscopic and analytical[4,10] results point to a species within the composition range $MoFe_{6-8}S_{8-10}$, whose structure is incompletely defined. FeMoco contains the biologically unique $S = {}^3/_2$ spin system which is the source of its distinctive EPR spectrum.[3] The features of the spectrum of free FeMoco are broader than those of the spectra of FeMo proteins. Treatment of FeMoco with ~1 equiv of benzene thiol results in a narrowing of these features so that the spectrum more closely resembles that of the FeMo protein.[11]

The most incisive structural information on FeMoco has come from X-ray absorption spectroscopy, XAS.[3] XAS is the general term used to refer to both the edge, near (or above) edge (XANES), and extended fine structure (EXAFS) regions of the X-ray absorption spectrum. The edge and XANES regions, collectively referred to in this paper as simply the XANES region, contain information about the geometric and electronic state of the absorbing atom. The EXAFS region provides metrical details about the coordination spheres surrounding the absorbing atom. Our original Mo EXAFS analyses on nitrogenase and its FeMoco,[12] which established the presence of Fe and S atoms within bonding distance of the Mo atom, have been extended with improved data and will be reported elsewhere.[13] Iron EXAFS[14] fully supports a cluster structure for FeMoco. As part of our continuing

(1) (a) Stanford University. (b) Battelle-Kettering Laboratory (contribution No. 870). (c) Western Regional Research Center, U.S. Department of Agriculture. (d) Purdue University. (e) Harvard University. (f) University of California, Irvine. (g) Department of Biochemistry and Biophysics, University of California, Davis, CA 95616. (h) Present address: Corporate Research Laboratories, Exxon Research and Engineering Co., Annandale, NJ 08801.

(2) Hawkes, T. R.; McLean, P. A.; Smith, B. E. *Biochem. J.* **1984**, *217*, 317.

(3) Abbreviations used: NMF, *N*-methylformamide; EPR, electron paramagnetic resonance; XAS, X-ray absorption spectroscopy; EXAFS, extended X-ray absorption fine structure; XANES, X-ray absorption near edge structure.

(4) (a) Shah, V. K.; Brill, W. J. *Proc. Natl. Acad. Sci. U.S.A.* **1977**, *74*, 3249. (b) Yang, S.-S.; Pan, W.-H.; Friesen, G. D.; Burgess, B. K.; Corbin, J. L.; Stiefel, E. I.; Newton, W. E. *J. Biol. Chem.* **1982**, *257*, 8042. (c) Burgess, B. K.; Newton, W. E. In "Nitrogen Fixation: The Chemical-Biochemical-Genetic Interface"; Müller, A., Newton, W. E., Eds.; Plenum Press: New York, 1983; pp 83–110.

(5) Mortenson, L. E.; Thorneley, R. N. F. *Annu. Rev. Biochem.* **1979**, *48*, 387.

(6) Eady, R. R.; Smith, B. E. In "A Treatise on Dinitrogen Fixation"; Hardy, R. W. F., Bottomley, F., Burns, R. C., Eds.; Wiley: New York, 1979; section II, chapter 2.

(7) Nelson, M. J.; Lindahl, P. A.; Orme-Johnson, W. H. *Adv. Inorg. Biochem.* **1982**, *4*, 1.

(8) Averill, B. A. *Struct. Bonding (Berlin)* **1983**, *53*, 59.

(9) (a) MCD spectra: Johnson, M. K.; Thomson, A. J.; Robinson, A. E.; Smith, B. E. *Biochim. Biophys. Acta* **1981**, *671*, 61. Robinson, A. E.; Richards, A. J. M.; Thomson, A. J.; Hawkes, T. R.; Smith, B. E. *Biochem. J.* **1984**, *219*, 495. (b) ENDOR: Hoffman, B. M.; Roberts, J. E.; Orme-Johnson, W. H. *J. Am. Chem. Soc.* **1982**, *104*, 860. Hoffman, B. M.; Venters, R. A.; Nelson, M.; Orme-Johnson, W. H. *Ibid.* **1982**, *104*, 4711.

(10) Nelson, M. J.; Levy, M. A.; Orme-Johnson, W. H. *Proc. Natl. Acad. Sci. U.S.A.* **1983**, *80*, 147.

(11) (a) Burgess, B. K.; Stiefel, E. I.; Newton, W. E. *J. Biol. Chem.* **1980**, *255*, 353. (b) Rawlings, J.; Shah, V. K.; Chisnell, J. R.; Brill, W. J.; Zimmermann, R.; Münck, E.; Orme-Johnson, W. H. *J. Biol. Chem.* **1978**, *253*, 1001.

(12) (a) Cramer, S. P.; Hodgson, K. O.; Gillum, W. O.; Mortenson, L. E. *J. Am. Chem. Soc.* **1978**, *100*, 3398. (b) Cramer, S. P.; Gillum, W. O.; Hodgson, K. O.; Mortenson, L. E.; Stiefel, E. I.; Chisnell, J. R.; Brill, W. J.; Shah, V. K. *J. Am. Chem. Soc.* **1978**, *100*, 3814.

(13) (a) Conradson, S. D.; Burgess, B. K.; Hodgson, K. O.; Mortenson, L. E.; Newton, W. E., results to be published. (b) Conradson, S. D., Ph.D. Thesis, Stanford University, 1983. (c) Certain results have been briefly presented: Burgess, B. K.; Yang, S.-S.; You, C.-B.; Li, J.-G.; Friesen, G. D.; Pan, W.-H.; Stiefel, E. I.; Newton, W. E.; Conradson, S. D.; Hodgson, K. O. In "Current Perspectives in Nitrogen Fixation"; Gibson, A. H., Newton, W. E., Eds.; Elsevier/North Holland: Amsterdam, 1981; pp 71–74.

(14) Antonio, M. R.; Teo, B.-K.; Orme-Johnson, W. H.; Nelson, M. J.; Groh, S. E.; Lindahl, P. A.; Kauzlarich, S. M.; Averill, B. A. *J. Am. Chem. Soc.* **1982**, *104*, 4703.

Mo XAS studies of nitrogenase, we have collected good quality Mo K-edge X-ray data of the dithionite-reduced state of the FeMo protein and both free and benzene thiol/selenol treated FeMoco. Corresponding data have also been collected for a variety of structural types of Mo compounds, including many synthetic Fe–Mo–S clusters, whose properties and utility as precursors and models for FeMoco have been described at some length.[8,15-17] These compounds[18-35] are given in Table I.   In this report, XANES of the natural and synthetic clusters are presented and compared. These results complement the EXAFS data, and together they provide a more detailed insight into the structure at the Mo site of the native cluster.

Experimental Section

Preparation of Samples. (a) Synthetic Fe–Mo–S Clusters. The compounds 1–15 listed in Table I were prepared by methods in the indicated references.

(b) FeMo Proteins and FeMoco. The FeMo protein of *C. pasteurianum* was prepared by a variation of a previous method.[36] The specific activity of the purified protein was 1810–1980 nmol of C_2H_2 reduced/ min/mg of protein. The sample solution had [Mo] $\simeq$ 1.5 mM and an atom ratio of Fe:Mo = 16:1. The FeMo protein of *A. vinelandii* was purified to homogeneity as described;[37] its specific activity was 2150

(nmol of C_2H_2 reduced/min/mg of protein). FeMoco was prepared from this protein by the large scale HCl/NaOH modification[4b] of the original isolation method.[4a] NMF extracts were concentrated by vacuum distillation[37] and were centrifuged to separate solid material. Sample solutions had [Mo] = 0.6–1.3 mM, Fe:Mo = 6.85–7.10, and activities in the UW45 reconstitution assays[4a] of 224–276 nmol of C_2H_2 reduced/ min/ng-atom of Mo. Solutions of FeMoco + PhSH or PhSeH contained 10 equiv of additive/mol of Mo. All sample solutions were 1–2 mM in $Na_2S_2O_4$. Sample integrity was monitored by activity determinations, which revealed <10% decrease after XAS measurements. Similarly, the EPR spectra were virtually unchanged after XAS measurements and corresponded to those of previous prepartions.[4b,11] The EPR spectrum of the FeMoco/PhSeH system was very similar to that containing PhSH[11] showing sharpening and small *g*-value shifts of the signals.

XAS Measurements. All data were acquired at the Stanford Synchrotron Radiation Laboratory under dedicated synchrotron radiation production conditions, with a two-crystal Si [220] monochromator detuned ~50% for reduction of the harmonic content of the beam. Spectra were calibrated with Mo foil, with the first inflection point in the edge absorption spectrum taken as 20003.9 eV. Synthetic compounds were measured as solids at ambient temperature. Spectra of FeMo protein and FeMoco samples were obtained in aqueous buffer at 2–4 °C and NMF solutions at -15--25 °C, respectively. Data on the solid samples were recorded in transmission mode with the compounds pressed into solid pellets, in some cases diluted with boron nitride or lithium carbonate. Data on solutions of the FeMoco and the protein were measured by the fluorescence technique by using an array of NaI (Tl) scintillation detectors with Zr filters.[38]   All measurements were performed under anaerobic conditions. Absorbance data were treated by subtraction of the extrapolated pre-edge absorbance, which was calculated by fitting a negative second-order polynomial through a several hundred eV wide, smoothly decreasing portion of the data prior to the onset of the Mo K-edge absorption discontinuity. First and second derivatives of the absorbance with respect to energy were obtained by differentiation of a third-order polynomial fit to the data over an interval of ±3.5 eV on each side of a data point. With the monochromator used, this corresponded to three data points on each side of a central point.

Method and Results

The X-ray absorption edge of an element appears as a sudden, discontinuous increase in absorbance superimposed upon a gradual decrease in absorbance as the photon energy increases. The X-ray absorption edge is normally taken to include that region of the spectrum extending from onset of the absorption discontinuity to the beginning of the EXAFS, ca. 25–50 eV higher in energy. At and just above the absorption threshold, transitions from core levels to higher lying bound atomic or molecular states give rise to structure on the absorption edge. At higher energies, transitions can occur into continuum states giving rise to additional structure that extends in energy to the onset of the EXAFS. This latter region contains what is classically called XANES, but for the presentation and interpretation of the data presented herein, it is more convenient to consider the whole edge region collectively and simply as XANES.

Experimental Considerations. The combination of lifetime broadening (~6.5 eV[39]) and monochromator band pass (~1 part in 10^4[40] or 2 eV minimum) results in a resolution of 6–8 eV at best for Mo K edges. With this resolution, edge transitions are not clearly resolved, and, therefore, experimental results are presented as the second derivative of the normalized absorbance with respect to energy ($\partial^2 A/\partial E^2$). This renders the structure of the XANES more apparent. Because the actual resolution is dependent upon the specific characteristics of the spectrometer, it is not exactly reproducible among different experimental sessions. Poorer resolution decreases the absolute amplitudes and the apparent separation of the features in $\partial^2 A/\partial E^2$. However, the relative amplitudes of features in $\partial^2 A/\partial E^2$ are not affected by either the resolution or, because of the low (<1.5) absorbances of all the samples, by the thickness effect.[41]   In addition, errors in the

(15) (a) Holm, R. H. *Chem. Soc. Rev.* **1981**, *10*, 455. (b) Holm, R. H.; Armstrong, W. H.; Christou, G.; Mascharak, P. K.; Mizobe, Y.; Palermo, R. E.; Yamamura, T. In "Biomimetic Chemistry" (Proceedings of the 2nd International Kyoto Conference on New Aspects of Organic Chemistry); Yoshida, Z.-I., Ise, N., Eds.; New York: Elsevier, 1983; pp 79–99.

(16) Coucouvanis, D. *Acc. Chem. Res.* **1981**, *14*, 201.

(17) Holm, R. H.; Simhon, E. D. In "Metal Ions in Biology"; Spiro, T. G., Ed.; Wiley-Interscience: New York, 1985; Vol. 7, Chapter 1, in press.

(18) McDonald, J. W.; Friesen, G. D.; Rosenhein, L. D.; Newton, W. E. *Inorg. Chim. Acta* **1983**, *72*, 205.

(19) (a) Kanatzidis, M. G.; Coucouvanis, D. *Acta Crystallogr., Sect. C: Cryst. Struct. Commun.* **1983**, *C39*, 835. (b) Lapasset, P. J.; Chezeau, N.; Belounge, P. *Acta Crystallogr., Sect. B: Struct. Crystallogr. Cryst. Chem.* **1976**, *B32*, 3087.

(20) Coucouvanis, D.; Stremple, P.; Simhon, E. D.; Swenson, D.; Baenziger, N. C.; Draganjac, M.; Chan, L. T.; Simopoulos, A.; Papaefthymiou, V.; Kostikas, A.; Petrouleas, V. *Inorg. Chem.* **1983**, *22*, 293.

(21) (a) Tieckelmann, R. H.; Silvis, H. C.; Kent, T. A.; Huynh, B. H.; Waszczak, J. V.; Teo, B.-K.; Averill, B. A. *J. Am. Chem. Soc.* **1980**, *102*, 5550. (b) Teo, B.-K.; Antonio, M. R.; Averill, B. A. *Ibid.* **1983**, *105*, 3751.

(22) Friesen, G. D.; McDonald, J. W.; Newton, W. E.; Euler, W. D.; Hoffman, B. M. *Inorg. Chem.* **1983**, *22*, 2202.

(23) Coucouvanis, D.; Simhon, E. D.; Baenziger, N. S. *J. Am. Chem. Soc.* **1980**, *102*, 6644.

(24) Coucouvanis, D.; Simhon, E. D.; Stremple, P.; Ryan, M.; Swenson, D.; Baenziger, N. C.; Simopoulos, A.; Papaefthymiou, V.; Kostikas, A.; Petrouleas, V. *Inorg. Chem.* **1984**, *23*, 741.

(25) Chen, G. J.-J.; McDonald, J. W.; Bravard, D. C.; Newton, W. E. *Inorg. Chem.* **1985**, *24*, 2327.

(26) Cramer, S. P.; Hodgson, K. O.; Stiefel, E. I.; Newton, W. E. *J. Am. Chem. Soc.* **1978**, *100*, 2748.

(27) (a) Stiefel, E. I.; Eisenberg, R.; Rosenberg, R. C.; Gray, H. B. *J. Am. Chem. Soc.* **1966**, *88*, 2956. (b) Cowie, M.; Bennett, M. J. *Inorg. Chem.* **1976**, *15*, 1584.

(28) (a) Wolff, T. E.; Power, P. P.; Frankel, R. B.; Holm, R. H. *J. Am. Chem. Soc.* **1980**, *102*, 4694. (b) Wolff, T. E.; Berg, J. M.; Power, P. P.; Hodgson, K. O.; Holm, R. H. *Inorg. Chem.* **1980**, *19*, 430.

(29) Wolff, T. E.; Berg, J. M.; Hodgson, K. O.; Frankel, R. B.; Holm, R. H. *J. Am. Chem. Soc.* **1979**, *101*, 4140.

(30) (a) Christou, G.; Garner, C. D. *J. Chem. Soc., Dalton Trans.* **1980**, 2354. (b) Acott, S. R.; Christou, G.; Garner, C. D.; King, T. J.; Mabbs, F. E.; Miller, R. M. *Inorg. Chim. Acta* **1979**, *35*, L337.

(31) Wolff, T. E.; Berg, J. M.; Holm, R. H. *Inorg. Chem.* **1981**, *20*, 174.

(32) Huang, L.; Lin, S. *Jiegou Huaxue* **1984**, *3*, 25.

(33) Armstrong, W. H.; Mascharak, P. K.; Holm, R. H. *J. Am. Chem. Soc.* **1982**, *104*, 4373.

(34) Mascharak, P. K.; Armstrong, W. H.; Mizobe, Y.; Holm, R. H. *J. Am. Chem. Soc.* **1983**, *105*, 475.

(35) Palermo, R. E.; Singh, R.; Bashkin, J. K.; Holm, R. H. *J. Am. Chem. Soc.* **1984**, *106*, 2600.

(36) Zumft, W. G.; Mortenson, L. E. *Eur. J. Biochim.* **1973**, *35*, 401.

(37) Burgess, B. K.; Jacobs, D. B.; Stiefel, E. I. *Biochim. Biophys. Acta* **1980**, *614*, 196.
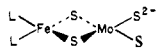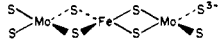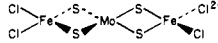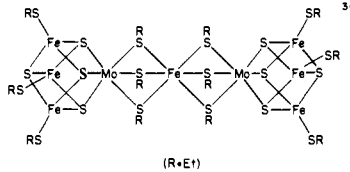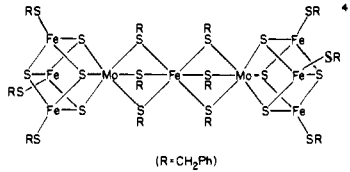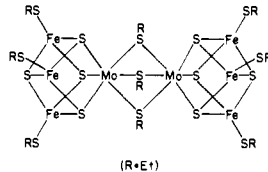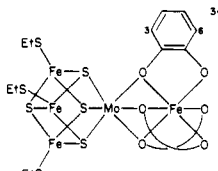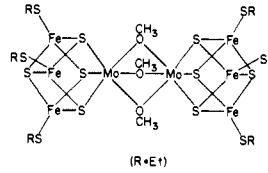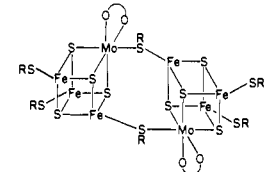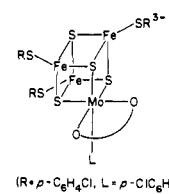
(38) Scott, R. A. In "Physical Techniques in Biological Research"; Rosseau, D., Ed.; Academic Press: New York, 1983; Vol. 2.

(39) Krause, M. O.; Oliver, J. H. *J. Phys. Chem. Ref. Data* **1979**, *8*, 329.

(40) Kincaid, B. M.; Eisenberger, P. *Phys. Rev. Lett.* **1975**, *34*, 1361.

(41) (a) Stern, E. A.; Bunker, B. A.; Heald, S. M. *Phys. Rev. B: Condens. Matter* **1980**, *21*, 5521. (b) Stern, E. A.; Kim, K. *Phys. Rev. B: Condens. Matter* **1981**, *23*, 3781.

Table I. Fe–Mo–S Compounds Examined by Mo K-Edge XANES

compound	structure	ref
Category I		
1, $(NH_4)_2[MoS_4]$	tetrahedral	18, 19
2, $(Et_4N)_2[(PhS)_2FeMoS_4]$	L = PhS⁻	20
3, $(Et_4N)_2[Cl_2FeMoS_4]$	L = Cl⁻	21
4, $(Et_4N)_3[Fe(MoS_4)_2]$		22, 23
5, $(Et_4N)_2[Cl_4Fe_2MoS_4]$		24
Category II		
6, $Mo(S_2CNEt_2)_2(S_2C_6H_4)$	distorted octahedral[a]	25, 26
7, $Mo(S_2C_6H_4)_3$	trigonal prismatic	27
8, $(Me_3NCH_2Ph)_3[Mo_2Fe_7S_8(SEt)_{12}]$	 (R=Et)	28
9, $(n\text{-}Bu_4N)_4[Mo_2Fe_7S_8(SCH_2Ph)_{12}]$	 (R=CH₂Ph)	29
10, $(Et_3NCH_2Ph)_3[Mo_2Fe_6S_8(SEt)_9]$	 (R=Et)	29, 30
Category III		
11, $(Et_4N)_3[MoFe_4S_4(SEt)_3(cat)_3]^b$		31
12, $(Et_4N)_3[Mo_2Fe_6S_8(SEt)_6(OMe)_3]$	 (R=Et)	30a, 32
Category IV		
13, $(Et_4N)_4[Mo_2Fe_6S_8(SEt)_6(al_2cat)_2]^c$	 (R=Et)	33
14, $(Et_4N)_3[MoFe_3S_4(S\text{-}p\text{-}C_6H_4Cl)_4(al_2cat)]^c$	 (R=p-C₆H₄Cl, L=p-ClC₆H₄S⁻)	34
Category V		
15, $(Et_4N)_3[MoFe_3S_4(S\text{-}p\text{-}C_6H_4Cl)_3(al_2cat)(CN)]^c$	as **14**, (R = $p\text{-}C_6H_4Cl$, L = CN⁻)	34, 35

[a] Assumed from EXAFS results;[26] X-ray structural determination has not been performed. [b] cat = catecholate. [c] al₂cat = 3,6-diallylcatecholate.
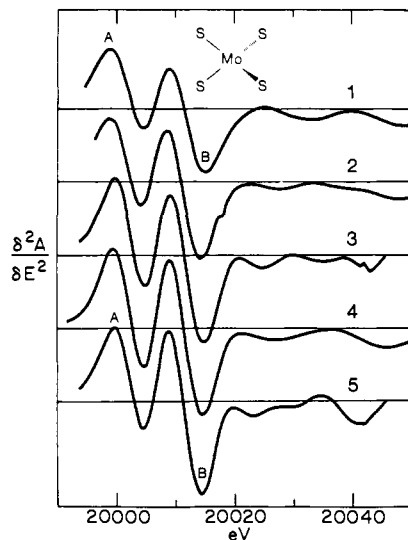
Figure 1. XANES spectra (presented as $\partial^2 A/\partial E^2$) of the Mo K absorption edge of category I compounds **1–5** (see Table I for structures). In certain of these and subsequent spectra sharp discontinuities (as in **2** and **3**) are experimental artifacts.
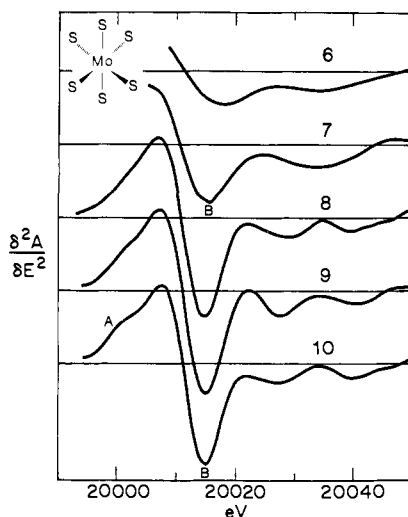

Figure 2. $\partial^2 A/\partial E^2$ of the Mo K absorption edge of category II compounds **6–10**. Spectra of **6** and **7** were not recorded to lower energies.

Figure 3. $\partial^2 A/\partial E^2$ of the Mo K absorption edge of category III compounds **11** and **12**.

Figure 4. $\partial^2 A/\partial E^2$ of the Mo K absorption edge of category IV compounds **13** and **14** (upper) and the category V compound **15** (lower).

spectral energies may be as large as several eV in some earlier spectra calibrated by taking periodic scans of a Mo foil and ±1 eV for more recently acquired data utilizing simultaneous calibrations.[42] The much weaker features above about 20 030 eV (ca. 18–20 eV above the inflection point of the principal absorption discontinuity) have not been used in the classification of compounds into classes based on $\partial^2 A/\partial E^2$ because of the presence of monochromator glitches in some spectra and because the greater sensitivity to noise in this region results in poor reproducibility of the spectra from some compounds.

Because of these considerations, conclusions based on the comparisons of $\partial^2 A/\partial E^2$ presented herein rely only on the presence or absence and the relative amplitudes of features in the region 20000–20030 eV and not the precise energies, absolute amplitudes, or more subtle differences in the shapes of these features.

XANES of Compounds. The Fe–Mo–S clusters investigated constitute an extensive set of both the linear and the cubane types, in which 2–4 sulfide and 1–3 Fe atoms are within bonding distances of the Mo atom. Certain of these species also contain RS^- and RO^- ligands coordinated to the Mo atom. Several mononuclear Mo–S complexes of different geometries complete this
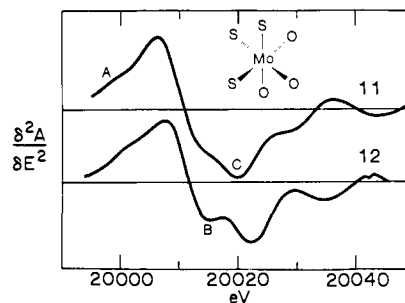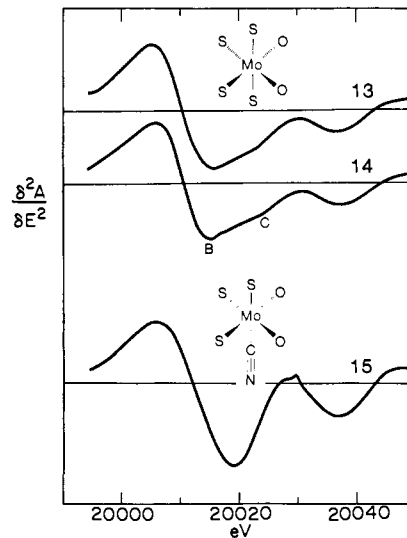
set. Except for **6**, structures of all members of the set (or close variants differing only in R substituents) have been determined by X-ray diffraction. Structural depictions and references to these determinations are included in Table I.

The XANES of the synthetic compounds fall into five distinct categories which correlate with certain attributes of their structures. Results for the different categories are first considered and then compared to the XANES of the FeMo protein and FeMoco. Plots of $\partial^2 A/\partial E^2$ vs. photon energy for these five categories are presented in Figures 1–4. Distances from the Mo absorber to other atoms quoted below are, where appropriate, mean values for a particular species. The symmetries refer only to the Mo site with respect to the first shell of nearest-neighbor atoms.

(a) **Category I.** Members of this subset contain as the common unit tetrahedral $[MoS_4]^{2-}$ (**1, 5**) distorted to C_{2v} symmetry (**2–4**). The Mo–S_b (2.21–2.26 Å) and Mo–S_t (2.15–2.17 Å) distances fall into fairly narrow ranges (b = bridging, t = terminal ligand). Spectral features (Figure 1) are identical within the experimental limitations up to 20 020 eV. Zero points occur near 20 004 and 20 011 eV, corresponding to the inflection points of a lower energy shoulder and the principal absorption edge discontinuity, respectively. Associated with these zeroes are two distinct minima, around which the shape of $\partial^2 A/\partial E^2$ is relatively symmetric, exhibiting no noticeable structure. Corresponding low energy features have been observed in the XANES of all compounds containing terminal Mo=O or Mo=S groups.[12a,43]

(b) **Category II.** This subset consists of the mononuclear complexes **6** (Mo–S, 2 S at 2.31 Å and 4 S at 2.42 Å[26]) and **7** (Mo–S, 2.37 Å) and the double cubanes **8–10**. In **8–10**, the Mo–μ_3S distances are 2.34–2.36 Å, and Mo–S_b distances are

(42) Scott, R. A.; Hahn, J. E.; Doniach, S.; Freeman, H. C.; Hodgson, K. O. *J. Am. Chem. Soc.* **1982**, *104*, 5364.

(43) (a) Kutzler, F. W.; Natoli, C. R.; Misemer, D. K.; Doniach, S.; Hodgson, K. O. *J. Chem. Phys.* **1980**, *73*, 3274. (b) Kutzler, F. W.; Scott, R. A.; Berg, J. M.; Hodgson, K. O.; Doniach, S.; Cramer, S. P.; Chang, C. H. *J. Am. Chem. Soc.* **1981**, *103*, 6083.

Mo XANES of Nitrogenase

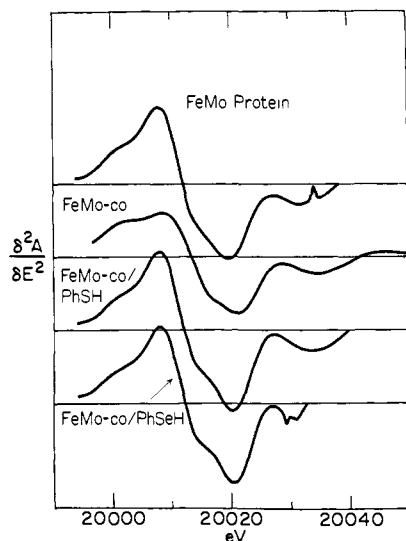*J. Am. Chem. Soc., Vol. 107, No. 26, 1985* 7939

Figure 5. $\partial^2 A/\partial E^2$ of the Mo K absorption edge of the dithionite-reduced FeMo protein of *C. pasteurianum*, FeMoco from the FeMo protein of *A. vinelandii*, FeMoco + PhSH, and FeMoco + PhSeH.

2.56–2.57 Å. The common feature of this category is the $Mo-S_6$ coordination unit, which is of D_{3h} symmetry in **7**, C_{3v} symmetry in **8–10**, and apparently of C_{2v} symmetry in **6**. The spectra shown in Figure 2 reveal a single zero at ca. 20 011 eV for all compounds corresponding to the inflection point of the principal absorption discontinuity. The shape of $\partial^2 A/\partial E^2$ is symmetric about the minimum, which occurs immediately past this zero. The large differences in the amplitude of the minimum between **6–7** and **8–10** are probably too large to be accountable in terms of resolution differences alone and may, therefore, be significant. Within the subset, the similarities of **8–10** in the shoulder at 20 003 eV (outside the range of the data from **6** and **7**) and in the experimentally less reliable region above 20 025 eV are apparent.

(c) **Category III.** This group consists of the single-cubane **11** and the methoxy-bridged dicubane, **12**, both with MoS_3O_3 coordination units of effective C_{3v} symmetry (Mo–O, 2.15–2.17 Å, Mo–μ_3S, 2.34 Å). In Figure 3, the zero of $\partial^2 A/\partial E^2$ corresponding to the inflection point of the principal absorption discontinuity occurs at 20 012–20 013 eV, which is slightly, but consistently, higher than those for category II and may result from the lower polarizability of the O ligands relative to S. The principal minimum beyond this is found at 20 020–20 023 eV. In contrast to previous cases, curve shapes about these minima are not symmetric and exhibit a shoulder or lesser minimum between the zero point and the principal minimum. Differences are also observed at higher energies. As for **8–10**, a weak shoulder near 20 000 eV is found.

(d) **Category IV.** Included in this category are the doubly bridged double cubane **13** and single cubane **14**. In **13**, subclusters are linked by two Mo–S(R)–Fe bridges with Mo–S_b = 2.69 Å. In **14**, one terminal ligand is a thiolate at a distance Mo–S = 2.60 Å. The Mo–O distances in the two clusters are 2.06–2.08 Å; the Mo–μ_3S distances are 2.36–2.38 Å. These clusters have nearly isometric MoS_4O_2 coordination units of effective C_s symmetry. The $\partial^2 A/\partial E^2$ curves for **13** and **14** (Figure 4) are essentially identical. The zeroes corresponding to the inflection points of the principal absorption discontinuities occur at 20 010–20 011 eV, and the following principal minima are found near 20 015 eV. Unlike previous clusters which had a symmetric minimum or a minimum preceded by structure at slightly lower energies, the spectra from this category show a poorly resolved shoulder on the high energy side of the minimum, near 20 023 eV. Beyond this point, the behavior resembles that of **12**.

(e) **Category V.** The cyanide-ligated cluster **15** with the MoS_3O_2C coordination unit (Mo–O, 2.12 Å; Mo–C, 2.19 Å; Mo–S, 2.38 Å; Mo–C–N, 178°) of C_s symmetry constitutes the only example in this category. Its XANES behavior is unique (Figure 4). The zero point corresponding to the inflection point

of the principal absorption discontinuity lies at 20 012 eV, with a rather symmetric curve shape around the minimum near 20 020 eV. This minimum is followed by a second zero crossing and a symmetric lesser minimum at 20 036 eV.

XANES of Nitrogenase. Shown in Figure 5 are $\partial^2 A/\partial E^2$ curves for the dithionite-reduced FeMo protein from *C. pasteurianum*, plus as isolated FeMoco, FeMoco + PhSH, and FeMoco + PhSeH from *A. vinelandii*. These resemble each other quite closely according to the classification criteria described previously. The zero which corresponds to the inflection point of the principal absorption discontinuity is at 20 012–20 013 eV, and the following minimum is at 20 018–20 020 eV. A shoulder occurs on the lower energy side of these minima in the 20 014–20 017 eV range, and a shoulder is evident near 20 000 eV. For the data sets presented, which were selected on the basis of the best apparent resolution, the spectra of FeMoco in the presence of PhSH and PhSeH are practically identical. In addition, they are far more similar to the spectrum of the FeMo protein than to that of untreated FeMoco. The XANES from the *A. vinelandii* FeMo protein (not shown) is identical within experimental error with that of the *C. pasteurianum* protein.

Discussion

In the absorption edge region, below the principal absorption maximum, spectral features arise from core-electron transitions to unoccupied molecular or atomic orbitals plus multielectron shakeup and shakedown processes. As shown by theoretical and experimental work on, e.g., Cu(II) compounds,[44] $[MoO_4]^{2-}$ and $[MoS_4]^{2-}$,[43a] and $[MoO_2S_2]^{2-}$,[43b] the assignment of these bound-state transitions is facilitated by having a viable theoretical model of the electronic structure or other property such as polarization dependence of the edge features.[43b,44b] This information is not yet available for the set of clusters in Table I.

Above the ionization threshold, the XANES is characterized by transitions to virtual, "inner", and "outer-well" states. Resonances in this region occur because, as opposed to the weak scattering which causes the EXAFS, the low kinetic energy photoelectron is strongly backscattered by the atoms in the vicinity of the absorber and can be considered as being momentarily trapped in multple-scattering resonances or in the relative minima in the molecular potential. This effect can, in some cases, render the XANES in this region sensitive to the higher order atomic correlations of the absorber environment, including more distant shells of atoms and bond angles.[45] The XANES is thus sensitive to the structure of the absorber site, which has resulted in the increased use of XANES as a source of structural information.[46]

Some general observations within the different subsets of Mo compounds are relevant to the influence of changes in structure on the XANES. For example, in the category I compounds, the $[MoS_4]^{2-}$ unit is coordinated to zero (in **1**), one (in **2**), or two (in **5**) FeX_2 moieties, *without* significant perturbation of the XANES up to about 20030 eV. In each of these cases, the first coordination shell around Mo contains four sulfur atoms in a tetrahedral or distorted-tetrahedral array. In category II, the trigonal prismatic complex, **7**, with six equivalent Mo–S bonds of 2.37 Å has XANES features very similar to the dicubane, **10**, which has three Mo–S bonds of ca. 2.35 Å and three of ca. 2.55 Å. However, when

(44) (a) Bair, R. A.; Goddard, W. A., III *Phys. Rev. B: Condens. Matter* **1980**, *22*, 2767. (b) Smith, T. A.; Penner-Hahn, J. E.; Berding, M. A.; Doniach, S.; Hodgson, K. O. *J. Am. Chem. Soc.* **1985**, *107*, 5945.

(45) (a) Durham, P. J.; Pendry, J. B.; Hodges, C. H. *Solid State Commun.* **1981**, *38*, 159. (b) Bianconi, A.; Dell'Ariccia, M.; Durham, P. J.; Pendry, J. B. *Phys. Rev. B: Condens. Matter* **1982**, *26*, 6502.

(46) (a) Belli, M.; Scafati, A.; Bianconi, A.; Mobilio, S.; Palladino, L.; Reale, A.; Burattini, E. *Solid State Commun.* **1980**, *35*, 355. (b) Bianconi, A.; Doniach, S.; Lublin, D. *Chem. Phys. Lett.* **1978**, *59*, 121. (c) Bianconi, A.; Giovannelli, A.; Castellani, L.; Alema, S.; Fasella, P.; Oesch, B.; Mobilio, S. *J. Mol. Biol.* **1983**, *165*, 125. (d) Tullius, T. D.; Gillum, W. O.; Carlson, R. M. K.; Hodgson, K. O. *J. Am. Chem. Soc.* **1980**, *102*, 5670. (e) Bunker, G.; Stern, E. A.; Blankenship, R. E.; Parson, W. W. *Biophys. J.* **1982**, *37*, 539. (f) Chance, B.; Powers, L.; Ching, Y.; Poulos, T.; Schonbaum, G. R.; Yamazaki, I.; Paul, K. G. *Arch. Biochim. Biophys.* **1984**, *235*, 596. (g) Müller, J. E.; Jepsen, O.; Andersen, O. K.; Wilkins, J. W. *Phys. Rev. Lett.* **1978**, *40*, 720.

the CN^- ligand is substituted to change the first coordination shell from MoS_4O_2 (in **13** or **14**) to $MoS_3O_2(CN)$, a clear change in the shape of the edge is seen. This edge perturbation is not unlike that observed for other π-bonding ligands such as CO.[47]

Association of XANES features with specific electronic and structural properties has been demonstrated.[44,46b,47] In this regard, we note the existence of features at "A", "B", and "C" which occur in more than one category (Figures 1–4) and could be indicative of transitions whose oscillator strengths are affected by the different structures exhibited by these compounds.

The feature at "A" in the edges of the category I compounds derives from a 1s $\rightarrow$ T_2 (ligand p and metal 4d) transition,[43] which becomes allowed in the noncentric tetrahedral point group. The smaller amplitude of the feature at A in categories II and III could result from the forbidden nature of this transition in these pseudo-octahedral Mo sites.

Features labeled "B" and "C" occur at energies higher than the principal absorption discontinuity. Transitions in this region involve transitions to continuum states and can be indicative of structural as well as electronic properties.[45,46c,f,g] The identification of even an empirical relationship between the relative intensities and the positions of these features in the XANES and structural features in these molecules might permit a more quantitative approach to the interpretation of the XANES of nitrogenase, requiring less recourse to model systems. However, such a correlation is difficult to quantitate in these data. The energy of the feature labeled "B" is consistent throughout all of the compounds in the different categories. The substitution of O (not terminally bound) for S in the coordination sphere of Mo generally results in a decrease of intensity in the "B" peak with enhancement in the features labeled "C". This pattern is seen in the edge of the category IV compounds which can be considered to have a coordination environment between those of categories II and III. However, the energy of the "C" peak varies among compounds both in category III and IV. It is, indeed, the relative change in intensity in the "B" and "C" regions which, coupled with the lack of the "A" feature, gives rise to the similarity between the spectra of the biological samples and compounds of category III. Unfortunately, the poor energy resolution and the lack of a theoretical description of the edges prevent quantitative understanding of these effects.

The validity of the information about the Mo site of nitrogenase obtained by this empirical correlation of the XANES is attested to by the obvious association between the XANES of **1–15** and the structures of the first shell of Mo atom nearest neighbors. In this relationship, the XANES appears to be more sensitive to the atoms and chemical nature of the bonds between the Mo and its neighbors and less sensitive to metrical and symmetry variations. In addition, the preceding discussion suggests that such interpretation be subject to the following qualifications: (i) close correspondence of the XANES from the sample of interest to that

from a standard implies structural and chemical similarity more than identity; (ii) a difference in the XANES is an unequivocal indication of a structural difference that may, however, involve only one nearest-neighboring atom or group; and (iii) structures inferred from interpolations (as opposed to direct comparisons) of the XANES of the unknown with the XANES and the structures of standards may be of dubious value.

On the basis of the comparisons of XANES of the synthetic compounds and the nitrogenase samples in the region 20000–20020 eV, the following unambiguous conclusions can be drawn concerning the Mo site structure in the enzyme and cofactor: (i) The Mo environment differs from those in **1–10** and **13–15**. (ii) The Mo site structure is most closely approached by **11** and **12**, which possess MoS_3O_3 coordination units with Mo–O bond lengths in the 2.1–2.2 Å range. This similarity indicates that the first shell of nearest neighbors to the Mo atoms in these states of nitrogenase consists of significant numbers of both singly bound hard and soft ligands. (iii) The Mo environments in the FeMo protein, FeMoco + PhSH, and FeMoco + PhSeH are more similar to each other than they are to FeMoco as isolated, but, by the XANES criterion, these differences are less pronounced than those which distinguish the different categories of synthetic compounds. Any changes in the structure resulting from the extraction of FeMoco from the protein and its subsequent reaction with PhSH/PhSeH must be sufficiently small so that the basic structure described in (ii) is conserved.

These conclusions based on XANES studies are completely consistent with and complementary to results from Mo EXAFS studies. Recent EXAFS studies[13] indicate that the coordination unit is $MoFe_{\sim 3}S_3O_3$ in FeMoco, $MoFe_{\sim 4}S_{4-5}O_2$ in the MoFe protein, and $MoFe_{\sim 4}S_4O_3$ in FeMoco + PhSh/PhSeH.[48] The Mo-neighboring atom distances are quite close to those in the cubane clusters such as those represented in categories II, III, and IV. Taken collectively, the XANES and EXAFS results provide convincing evidence that the Mo in nitrogenase is contained in a polynuclear Fe,S cluster with additional low Z ligation. The full set of EXAFS results will be published elsewhere.[13a]

---

(47) Kutzler, F. W.; Hodgson, K. O.; Doniach, S. *Phys. Rev. A* **1982**, *26*, 3020.

(48) These results are expressed in terms of oxygen content; however, oxygen and nitrogen are not distinguished by the EXAFS. The possibility of a $Mo^{VI}O$ group in the natural cluster has been eliminated owing to the absence of a characteristic pre-edge transition.[12]